Journal of Undergraduate Chemistry Research, **2025**, 24 (3), 78

MUTATIONAL STUDY OF SUBUNIT *a* RESIDUE, ASP124, OF *E. coli* ATP SYNTHASE

Kimberly V. Hoang*, Madison C. Stonestreet*, Cullen D. Martin*, Katherin E. Socias Baez*, David Emeka-Ibe* and Rashmi K. Capece†

Chemistry Department, Berea College, Berea, KY 40404

Abstract

F_1F_0 ATP synthase is a biological motor that couples ion translocation across a membrane to synthesis of ATP, the universal biological energy carrier. Proton movement through the F_0 motor induces conformational changes in the F_1 motor, catalyzing ATP production. While analyzing structures of *E. coli* ATP synthase, we identified a hydrogen-bonding network within the *a*-*b* interface formed by *a*Asp124, *a*Tyr11, *a*His15, and *b*Gln10. To understand the functional importance of *a*Asp124, we constructed three substitution mutations and studied their impact on *in vivo* oxidative phosphorylation and in vitro ATP synthesis and hydrolysis activities. The substitutions with non-polar and polar residues showed moderate to no loss of activities; however, introducing a longer side chain caused a significant defect, suggesting that the charge of *a*Asp124 may be unimportant for the ATP synthase functions.

†Corresponding author: capecer@berea.edu *Undergraduate researchers and underlined co-authors contributed equally to this work
Keywords: ATP synthase, oxidative phosphorylation, hydrogen-bonding, *Escherichia coli*
Received: August 1, 2025 Accepted: August 4, 2025 Revision received: August 4, 2025 Published: August 4, 2025

Introduction

Adenosine triphosphate (ATP) is the energy currency of all forms of life, produced by an enzyme called F_1F_0 ATP synthase by using a metabolically-driven electrochemical (H^+ or Na^+) gradient in the final step of oxidative phosphorylation.[1] It is found in the bacterial plasma membrane, mitochondrial inner membrane, and chloroplast thylakoid membrane. ATP synthase is central to energy production and pH regulation in the cell, making it an attractive drug target, particularly against multidrug-resistant bacteria.[2-3] It is a multi-subunit protein complex comprised of two rotary motors: a membrane-extrinsic F_1 motor, and a membrane-embedded F_0 motor. *Escherichia coli* F_1F_0 ATP synthase has the simplest subunit composition, consisting of eight protein subunits, and is used as a model system.[4,5] The F_1 domain consists of the γε central stalk surrounded by the $\alpha_3\beta_3$ hexamer with three active sites for ATP synthesis or hydrolysis, and cap δ positioned on top of the hexamer. The F_0 domain contains the rotor ring of 10 *c* subunits, asymmetrically wrapped by subunit *a* and the peripheral stalk formed by a homodimer of subunits *b*. Ion translocation through the *a*-*c* interface drives *c*-ring rotation that is coupled to the rotation of the γ stalk, which in turn induces conformational changes in the $\alpha_3\beta_3$ hexamer, triggering ATP synthesis by the binding change mechanism.[6,7] Conversely, depending on the physiological demand of the living cell, ATP synthase can hydrolyze ATP to pump protons in the reverse direction.[1]

The b_2 dimer in *E. coli* is crucial for binding F_1 to F_0 and linking ion translocation through F_0 with catalytic activity in F_1.[1,8] It forms an elongated coiled-coil structure, in which the N-terminal region resides within the cell membrane (F_0) and the C-terminal region interacts with the δ subunit of the F_1 domain. Just above the membrane, the dimer splits into two helices that straddle subunit *a*, which is composed of five transmembrane (TM) helices. This arrangement enables b_2 to bind to two regions of subunit *a*.[4] However, the key interaction sites between *a* and *b* subunits are not clear. The functional impact of deletion of the N-terminal region of TM helix 1 of subunit *a* suggested its interaction with *b* subunits.[9] Additionally, recent cryo-electron microscopy structures of *E. coli* ATP synthase show that the TM 2-3 periplasmic loop of subunit *a* forms an interface with one of the *b* subunits, here referred as b_i.[4, 10-11] A similar periplasmic loop is also present next to the *b* subunit of *Bacillus* PS3 ATP synthase, and it was proposed that the loop may interact with the N-terminus of *b* on the periplasmic side.[12] Densities of lipid-chains have also been identified as a part of the *a*-b_i interface in *E. coli*.[11] Moreover, analyses of the cryo-electron microscopy models of *E.coli* ATP synthase in different rotational states showed a hydrogen-bonding network formed at the *a*-b_i interface as presented in Figure 1, comprised of Tyrosine 11 (*a*Tyr11, a residue from N-terminus of subunit *a*), Aspartate 124 (*a*Asp124, a residue located in the TM 2-3 periplasmic loop), Histidine 15 (*a*His15, a residue considered important for the assembly of F_0 domain)[13], and Glutamine 10 of subunit b_i (*b*Gln10). Out of the seventeen structures analyzed, fifteen showed that the side chain of *a*Asp124, formed a hydrogen bond with the side chain of *b*Gln10. Additionally, all structures showed that *a*Asp124 hydrogen bonded with *a*Tyr11 and fourteen of them showed hydrogen bonding with *a*His15. A hydrogen-bonding network is also present at one

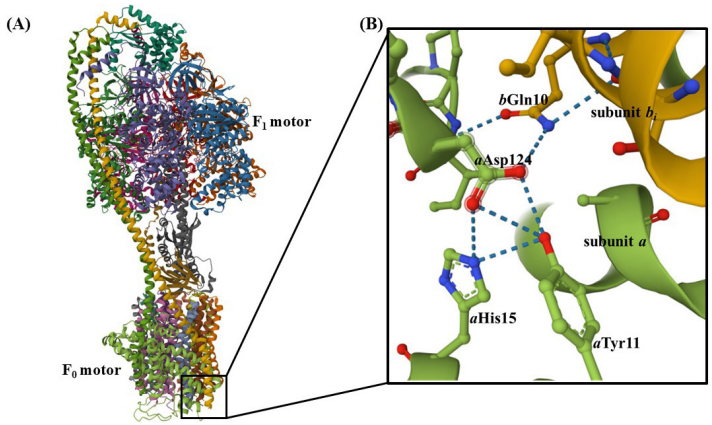

Figure 1. E. coli ATP synthase (PDB 6OQW)[11]. A) Ribbon representation of F_1F_0 ATP synthase indicating the *a*-b_i interface in the F_0 domain. B) Expanded view of the hydrogen-bonding network formed by Tyr11, His15 and Asp124 of subunit *a* with Gln10 of subunit b_i. Subunit *a* is shown in green and subunit b_i in yellow. Hydrogen bonds are shown in blue dashes. This figure is generated using Mol*.[22-23]

of the αβ interfaces in the F_1 domain, and its elimination resulted in the severe dysfunction.[14] Since *a*Asp124 is involved in forming multiple hydrogen bonds with its neighboring residues, we studied the functional importance of the chemical properties of this residue. We performed three substitution mutations at *a*Asp124 to examine the impacts of polarity, charge, and size changes on ATP synthase function.

Experimental Methods

Reagents and strains

De novo synthesized gene fragments of all mutants were purchased from Twist Bioscience (South San Francisco, CA) and the primers for polymerase chain reaction were obtained from Integrated DNA technologies (Coralville, IA). The restriction enzymes BsrGI and PflMI were obtained from New England Biolabs (Ipswich, MA). The plasmid construct pRFV2 and *unc* (atp) operon deleted *E. coli* strain DK8 were kindly provided by Prof. Ryan Steed, University of North Carolina at Asheville. The plasmid pRFV2 consists of genes encoding all eight subunits of *E. coli* F_1F_0 ATP synthase with cysteines in F_1 substituted with alanine and the single cysteine in subunit *b* of F_0 substituted with serine. The source of wildtype (WT) ATP synthase is plasmid pRFV2.

Construction of Mutations

Commercially bought mutant gene fragments were amplified by polymerase chain reaction using the forward primer (5' CATAGGACACCACCTGAATAACCTTCAG 3') and the reverse primer (5' CCGATCGCAGCACCGATTGCCGCCAGACCC 3'). The amplified mutant fragments were then digested using the restriction enzymes and ligated into the cut plasmid pRFV2 at the BsrGI and PflMI restriction sites. The presence of mutations was confirmed by Sanger sequencing using the primer 5' CACACGCAGTGCAGGCAGACCCAGTACATG 3'. Then the plasmids with the desired mutations were transformed into DK8 (*Δunc*) strain.[15]

Growth Assay in minimal media

Growth of WT and mutant DK8 transformant strains in limiting glucose and succinate M63-TIV minimal medium (61.8 mM KH_2PO_4, 38.2 mM K_2HPO_4, 15 mM $(NH_4)_2SO_4$, 1 mM MgSO4, 1 µg/mL thiamine, 0.2 mM isoleucine, 0.2 mM valine) were measured following the modified assay.[16] Each strain was streaked on an Luria Broth (LB) agar plate with 100 µg/mL ampicillin and a single colony was inoculated using 3 ml M63-TIV minimal medium with 0.1% (w/v) glucose and 5% (v/v) LB, which was then grown at 37°C overnight. The cell density of the overnight culture was measured by obtaining the absorbance at 550 nm, which was then used to inoculate 1 mL M63-TIV minimal medium with 0.04% (w/v) glucose or 0.6% (w/v) succinate such that the cell density was about 0.08. The growth media contained 100 µg/mL ampicillin except when culturing the negative control, the untransformed DK8 (*Δunc*). 300 µL of the culture was loaded in a clear 96-well microplate and placed in BioTek Synergy HTX multimode reader. Growth was monitored over 12 hours at 37 °C with shaking by measuring the cell density at 550 nm every 30 minutes. Maximum cell density during the growth period of 12 hours was determined, subtracted by the blank and normalized to wildtype. The experiment was replicated three-six times.

Inverted membrane vesicle preparation

Both WT and mutant DK8 transformants were grown in 1 L LB media at 37˚C overnight, shaking at 170 rpm. When the cell density of the culture reached 0.8, cells were harvested by centrifugation at 4500 rpm for 20 minutes at 4ºC. The pellets were then resuspended in TMG buffer (50 mM Tris-acetate, 5 mM $MgCl_2$, 10% v/v glycerol, pH 7.5) supplemented with 1 mM dithiothreitol and 1 mM phenylmethanesulfonyl fluoride and passed through an Avestin Emulsiflex B15 homogenizer operating at ≥ 15000 psi three times. The lysate was collected and centrifuged at 9,000 x g for 10 minutes at 4°C to remove cellular debris and intact cells. The cleared fraction was then further centrifuged at 209,438 × g at 4°C for 30 minutes. Membrane pellets were washed once and resuspended in TMG buffer using a Dounce homogenizer. The vesicles were stored at -80°C and later were analyzed using the modified Lowry method with bovine serum albumin as a standard.[17]

ATP synthesis assay

A modified luciferin/luciferase assay was used to measure ATP synthesis.[20] A reaction mixture (5 mM Tricine, pH 8.0, 50 mM KCl, 2.5 mM $MgCl_2$, 3.75 mM potassium phosphate, 0.1 mM adenosine diphosphate, 2.5 mM reduced β-nicotinamide adenine dinucleotide (NADH), 125 µM luciferin, and 100 ng luciferase) of 280 µL was added in a 96-well white microplate. Then 20 µL of 0.5 mg/mL inverted membrane vessels were added to start the reaction. Using a BioTek Synergy HTX microplate reader, luminescence was measured every 3s for 5 min at 30°C. The relative luminescence was calculated using the slope of 10 initial consecutive points during the assay. Each assay was performed four times.

ATP hydrolysis assay

ATP hydrolysis was determined using a calorimetric method in which the inorganic phosphate released during the reaction was measured as described previously.[19] In a 3 mL test-tube containing 1.8 mL ATPase cocktail (10 mM NaATP, 4 mM $MgCl_2$, and 50 mM Tris-SO_4 pH 8.5), 60 µg of inverted membrane vesicle was added and incubated at 37˚C to allow hydrolysis reaction to occur. At each interval (5, 10, 15, 20, and 25 min) 300 µL aliquots from the reaction mixture were removed, which was then added to 300 µL of 10% SDS to stop the reaction and placed on ice. For a zero-time point, 300 µL of 10% SDS was added to the 300 µL ATPase cocktail and 10 µg of the vesicle was added to prevent the reaction process. After that, 300 µL of Taussky and Shorr reagent[20] was added to each mixture, which reacts with the inorganic phosphate produced from the reaction, giving a blue coloration. The absorbance was then measured at 700 nm using a BioTek Synergy HTX microplate reader. The relative absorbance was calculated using the slope of six consecutive points. The experiment was performed in triplicates.

All data, including statistical analysis using t-test, were performed in Microsoft Excel.

Results

Mutations of Asp124

Three substitution mutants of *a*Asp124 were created to test our hypothesis that hydrogen bonds formed by *a*Asp124 with its neighboring residues including *b*Gln10 at the a-b_i interface have functional importance. We constructed non-polar residue Alanine

(Ala) and polar residue Cysteine (Cys) mutations to assess whether altering the polarity and neutralizing the charge would affect hydrogen bonding. Mutation to Glutamate (Glu) evaluated if the other negative charge could maintain the hydrogen bonding or the size would impact the role of Asp.

Growth on limited glucose and succinate medium

To determine whether these mutations affected oxidative phosphorylation *in vivo*, all mutants were grown on M63-TIV minimal medium supplemented with limited glucose or succinate, as the only carbon source. Oxidative phosphorylation is important for the growth of *E. coli*. The results are shown in Figure 2. All mutants grew well on 0.04% (w/v) glucose minimal medium except Asp124Glu ($p < 1.0 \times 10^{-5}$), whose growth was lower than the negative control, Δ*unc*. Similarly, on the succinate minimal medium, both Asp124Cys and Asp124Ala showed no significant growth defect, but Asp124Glu had the most growth defect ($p < 1.0 \times 10^{-7}$) compared to the WT. We expected no growth for Δ*unc* strain in succinate minimal media. However, the 20% growth seen in Δ*unc* may have to do with the residual LB and glucose of the overnight culture used to inoculate the media.

NADH-driven ATP synthesis activity

The efficiency of the inverted membrane vesicles of mutant strains was investigated by NADH-driven ATP synthesis activity. The results are shown in Figure 3. The introduction of a polar neutral residue Cys and a non-polar neutral residue Ala showed no significant effect on synthesis activity. Surprisingly, Asp124Glu with similar charge but an extra methylene group caused a significant activity defect ($p < 0.003$).

ATP hydrolysis activity

The effect of mutations on ATP hydrolysis was examined by the production of inorganic phosphate as described above. The results are shown in Figure 4. Both Asp124Cys and Asp124Ala had similar hydrolysis activity like WT while Asp124Glu had the lowest activity overall. However, the effect of Asp124Glu on the hydrolysis activity was statistically insignificant.

Discussions

In this study, we demonstrated that the charge of *a*Asp124 residue is not the critical attribute for the function of ATP synthase. The side chain carboxylate group of *a*Asp124 can form a hydrogen bond with the hydroxyl group of *a*Tyr11, the imidazole of *a*His15 and side chain amide of *b*Gln10. Neutralizing the charge via the

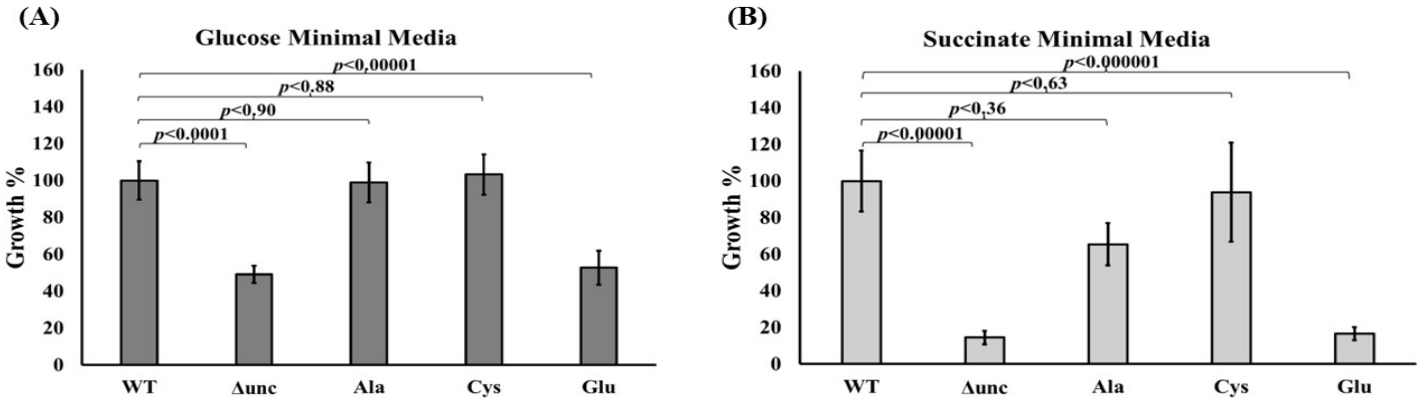

Figure 2. Growth of mutants on minimal medium. The growth of WT, negative control (Δunc) and Asp124 mutants on M63-TIV minimal medium containing (A) 0.04% glucose or (B) 0.6% succinate was monitored by measuring cell density at 550 nm. The maximum cell density during the 12 hours growth period was normalized to WT. Results presented are averages of n≥3 ± standard error with p-values relative to WT.

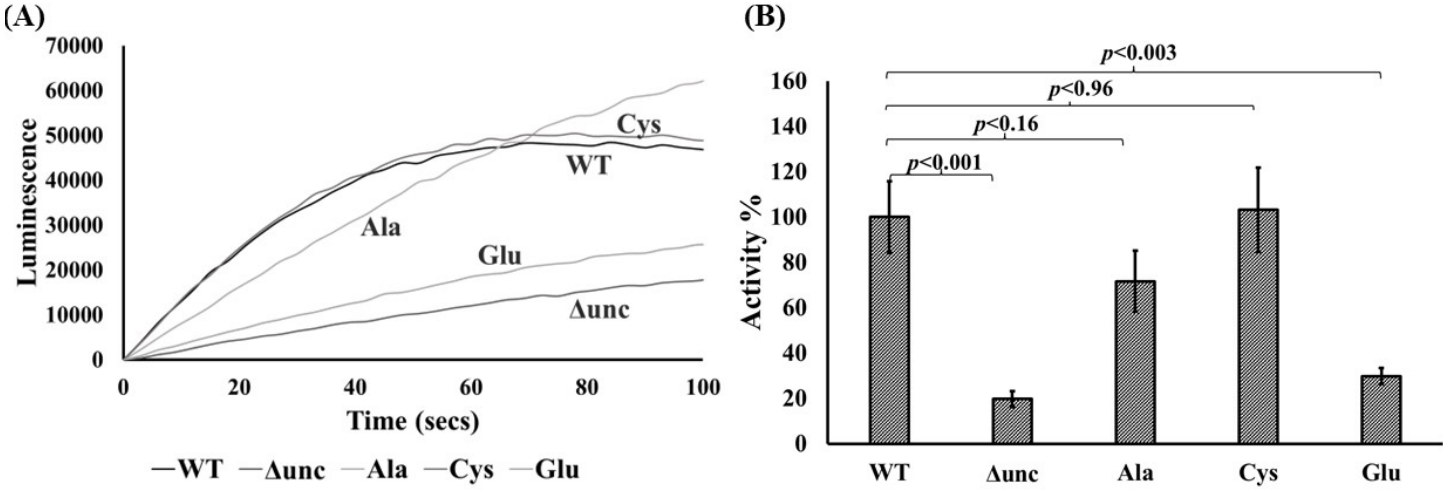

Figure 3. ATP synthesis by Asp124 mutants: (A) A real-time measurement of ATP synthesis driven by NADH and proton gradient. The inverted membrane vesicles were energized by NADH at t=0 and luminescence was monitored for 5 mins (300 secs) at 37°C. Only the luminescence of the first 100 secs is shown here. (B) Activities of mutants are plotted relative to WT. Bar represents the maximum slope defined by the first 10 consecutive points. Activities are plotted as mean ± standard error with p-values. Results are the averages of n≥3 experiments.

*a*Asp124Cys mutant did not affect the synthesis or hydrolysis activities of ATP synthase. On the other hand, eliminating all potential hydrogen bonds formed by the side chain of *a*Asp124 in the *a*Asp124Ala mutant did not significantly affect the enzyme activities, suggesting that the hydrogen bonds formed by the *a*Asp124 may be unimportant for the functionality of the enzyme. However, maintaining the negative charge but adding an extra methylene group in the *a*Asp124Glu mutant was detrimental to all activities compared to other mutants, suggesting a potential steric clash with the neighboring residues due to the longer side chain. Overall, the results show that it is not polarity but sterics in the *a*-b_i interface that has the most significant effect on ATP synthase activities.

This effect of the *a*Asp124Glu mutation could arise due to the disruption between lipid and peripheral stalk interactions. Lipid densities are observed in multiple locations of the F_0 motor, mainly within the *a*-*c* interface, which are suggested to strengthen the connections between the interacting surfaces.[11] Additionally, a weaker density of lipid-chains near the periplasmic loop of subunit *a* and b_i interface was also identified.[11] The longer chain of Glu could clash with the non-polar chains of the lipids affecting lipid-b_i interactions and the stability of the b_i peripheral stalk. This unstable subunit *b* can interrupt the coupling between F_1F_0, resulting in the loss of function.

The other possibility is that the *a*Asp124Glu mutation affects the assembly of the F_0 domain, as seen in *a*His15Asp mutation. *a*His15Ala showed little to no effect in the function of the ATP synthase; however, *a*His15Asp mutation caused loss of assembly as detected by the low level of subunit *a*, subsequently uncoupling F_1F_0.[13] The F_0 domain is formed when subunits *a*, *b* and *c* are inserted into the membrane. In *E. coli*, the insertion of subunit *a* in the membrane requires the presence of both subunit *b* and *c*.[21] In the *a*His15Asp mutant, the presence of two like charges including *a*Asp124 may cause electrostatic repulsion affecting the structural integrity of subunit *a*, hence preventing the insertion of subunit *a* and assembly of the F_0 domain. Likewise, the *a*Asp124Glu mutation may also affect the structural integrity of subunit *a* by clashing with the neighboring residues, further affecting F_0 assembly. Furthermore, the isolated F_1 domain can catalyze the hydrolysis of ATP, but not its synthesis. Compared to synthesis, the higher activity of ATP hydrolysis shown by *a*Asp124Glu suggests the possibility of uncoupled F_1F_0. Further experiments such as immunoblotting of subunit *a* and ATP hydrolysis activity in presence of F_0 inhibitor are required to confirm the adverse effect caused by the longer side chain at position 124.

Conclusion

We have shown that hydrogen bonds formed by *a*Asp124 are not absolutely essential for the functions of ATP synthase. However, the introduction of longer side chain amino acid at position 124 reduces synthesis and hydrolysis activities. In the future, we will confirm the uncoupling of F_1F_0 and explore if the defects are due to weakened lipids and subunit *b* interaction or assembly of F_0.

Acknowledgements

The authors would like to acknowledge ORAU Ralph E. Powe Junior Faculty Enhancement Award and Berea College Undergraduate Research and Creative Projects Program for funding this research. We would also like to thank Berea College Biology Department for the use of Thermocycler and BioTek Synergy HTX microplate reader.

References

1. Kühlbrandt, W. *Annu. Rev. Biochem*. **2019**, *88*, 515-549.
2. Nesci, S.; Trombetti, F.; Algieri, C.; Pagliarani, A. *SLAS Discov*. **2019**, *24*, 893-903.
3. Hards, K.; Cook, G.M. *Drug Resis. Updat*. **2018**, *36*, 1-12.
4. Sobti, M.; Zeng, Y. C.; Walshe, J.L.; Brown, S.H.J.; Ishmukhametov, R.; Stewart, A. G. *Commun. Biol*. **2023**, 6.
5. Capaldi, R. A.; Schulenberg, B.; Murray, J.; Aggeler. *J. Exp. Biol.* **2000**, *203*, 29–33.
6. Walker, J.E. *Biochem. Soc. Trans*. **2013**, *41*, 1-16.
7. Boyer, P.D. Annu. Rev. Biochem. **1997**, *66*, 717-749.
8. Colina-Tenorio, L.; Dautant, A.; Miranda-Astudillo, H.; Giraud, M.F.; Gonzalez-Halphen, D. *Front. Ohysiol*. **2018**, *9*.
9. Ishmukhametov, R.R.; Deleon-Rangel, J.; Zhu, S.; Vik, S.B. *J.*

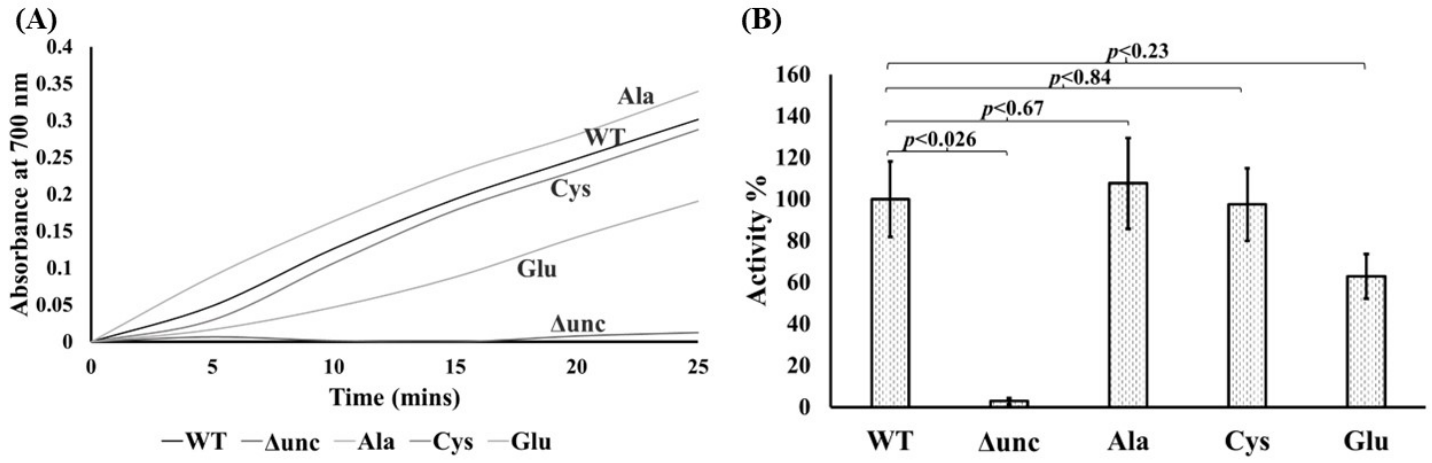

Figure 4. ATP hydrolysis by Asp124 mutants: (A) A time-point hydrolysis assay showing the absorbance of inorganic phosphate produced by the reaction. Each reaction mixture contained 10 µg of the inverted membrane vesicles mixed with ATPase cocktail and the reaction proceeded for 25 mins at 37°C before quenching with 10% SDS. (B) Activities of mutants are plotted relative to WT. Bar represents the slope of the absorbance of five time points. Activities are plotted as mean ± standard error with p-values. Results presented are averages of n≥3 experiments.

Bioenerg. Biomembr. **2017**, *49*, 171-181.
10. Sobti, M.; Smits, C.; Wong, A.S.; Ishmukhametov, R.; Stock, D.; Sandin, S.; Stewart, A.G. *eLife*. **2016**, *5*, e21598.
11. Sobti, M.; Walshe, J.L; Wu, D.; Ishmukhametov, R.; Zeng, Y.C.; Robinson, C.V.; Berry, R.M.; Stewart, A.G. *Nat. Commun*. **2020**, *11*.
12. Guo, H.; Suzuki, T.; Rubinstein, J. L. *eLife*. **2019**, *8*, e43128.
13. Patterson, A.R.; Wada, T.; Vik, S.B. *Arch. Biochem. Biophys*. **1999**, *368*, 193–197.
14. Mao, H.Z.; Abraham, C.G.; Krishnakumar, A.M.; Weber, J. *J. Biol. Chem*. **2008**, *283*, 24781-24788.
15. Klionsky, D.J.; Brusilow, W.S.; Simoni, R.D. J. Bacteriol. **1984**, *160*, 1055–1060.
16. Shrestha, R.K.; Founds, M.W.; Shepard, S.J.; Rothrock, M.M.; Defnet, A.E.; Steed, P.R. *Biochim Biophys Acta Bioenerg.* **2023**, *1864*.
17. Fillingame, R. *J. Bacteriol*. **1975**, *124*, 870-883.
18. Preiss, L.; Langer, J.D.; Yildiz, Ö.; Guillemont, J.E.G.; Koul, A.; Meier, T. *Sci. Adv.* **2015**, *1*.
19. Zulfiqar, A.; Laughlin, T.F.; Kady, I.O. *PLoS ONE*. **2015**, *10*, e0127802.
20. Taussky, H.H.; Shorr, E. *J Biol Chem.* **1953**, *202*, 675–685.
21. Hermolin, J.; Fillingame, R.H. *J Biol Chem.* **1995**, *270*, 2815–2817.
22. Sehnal, D.; Bittrich, B.; Deshpande, M.; Svobodová, R.; Berka, K.; Bazgier, V.; Velankar, S.; Burley, S.K.; Koča, J.; Rose, A.S. *Nucleic Acids Res.* **2021**, *49*, W431-W437.
23. Berman, H.M.; Westbrook, J.; Feng, Z.; Gilliland, G.; Bhat, T.N.; Weissig, H. Shindyalov, I.N.; Bourne, P.E. *Nucleic Acids Res.* **2000**, *28*, 235-242.